

Volatile, Trace, and Ore Elements in Magmatic Melts and Natural Fluids: Evidence from Mineral-Hosted Inclusions. II. Effect of Crystallization Differentiation on the Concentrations of Ore Elements

V. B. Naumov^{a, *}, A. V. Girnits^{b, **}, V. A. Dorofeeva^a, and V. A. Kovalenker^b

^a Vernadsky Institute of Geochemistry and Analytical Chemistry, Russian Academy of Sciences, Moscow, 119991 Russia

^b Institute of Geology of Ore Deposits, Petrography, Mineralogy, and Geochemistry, Russian Academy of Sciences, Moscow, 119017 Russia

*e-mail: naumov@geokhi.ru

**e-mail: girnits@igem.ru

Received March 24, 2021; revised October 6, 2021; accepted October 16, 2021

Abstract—In the second part of this study, we analyze how crystallization differentiation can affect concentrations of elements and their ratios in melt inclusions and glasses of rocks in major geodynamic environments. The paper presents analysis of experimental data on the partition coefficient of elements between minerals (olivine, pyroxenes, garnet, amphibole, biotite, sulfide, apatite, spinel, ilmenite, rutile, and zircon) and silicate melts, which were discussed in the first part of this study. It is demonstrated that the crystallization of major minerals only insignificantly affects the ratios of incompatible elements. The partition coefficients of some elements between accessory minerals and melts can be very high, but the effects of crystallization differentiation cannot be significant because of the small amounts of the crystallizing phases. These effects are the most significant for chalcophile elements (Cu, Ni, and others), at the separation of sulfides, and for Nb and Ta, at the crystallization of rutile. Differences in concentrations of various elements and their ratios to Cs concentrations are discussed with reference to various geodynamic environments. The maximum values of the ratios of practically all elements to Cs were found in melts in mid-oceanic ridges. The melts of oceanic islands and backarc basins are characterized by relatively low ratios, without any significant anomalies. The lowest ratios of elements to Cs were found in melts of continental and marginal environments. These melts are also characterized by clearly seen geochemical anomalies that are typical of rocks of the corresponding environments (negative Ta–Nb, positive Pb, and other anomalies).

Keywords: melt inclusion, partition coefficient, crystallization differentiation, accessory minerals

DOI: 10.1134/S0016702922060040

INTRODUCTION

In the first part of this study (Naumov et al., 2022; referred to as *Part I* below), we have evaluated the average compositions of melts from various geodynamic environments based on data on melt inclusions and glasses in rocks. These evaluations led us to reveal similarities and differences between melts from different environments in terms of concentrations of 45 volatile, trace, and ore elements. However, because chemical analyses of glasses presented in the literature pertain to melts that had been variably differentiated, the evaluated average compositions and ratios of elements cannot be directly used to deduce geochemical characteristics of the parental magmas and their sources (Kovalenko et al., 2007). In view of this, below we discuss how crystallization differentiation processes can affect geochemical characteristics of the melts. We will do this using data on melt inclusions

and glasses (Part I) and published experimental data on the partition coefficients of elements between minerals and silicate melts.

An inherent feature of ore elements at magma crystallization is that the behavior of these elements strongly depends on accessory minerals, whose accumulation is often the dominant factor that controls the origin of economic ores. We will discuss the possible effects of the crystallization of ore minerals (spinel, ilmenite, apatite, rutile, zircon, and sulfides) on the composition of magmas in comparison with the effects of rock-forming minerals. The effects related to the separation of fluid phases and to contamination are not discussed in this paper.

The significant role of accessory minerals in processes of crystallization differentiation is predetermined by the following two aspects. First, the contents of these elements are low because of the low concen-

trations of the dominant elements of the accessory phases (S for sulfides, Ti for ilmenite and rutile, P for apatite, Zr for zircon, etc.). The maximum amounts of accessory minerals crystallizing from primary melts can be estimated from the average concentrations of these elements in dominant melts. These estimates vary from 4 wt % for ilmenite to $\ll 1$ wt % for zircon. Note that the content of biotite, a phase that is commonly not viewed as an accessory mineral, is limited by the initial concentration of potassium in the melt. Mafic melts contain ~ 0.4 wt % K_2O , which corresponds to no more than 4 wt % biotite crystallizing from this melt. Because of this, biotite will be discussed below together with accessory minerals. Another feature of accessory minerals is that the partition coefficients of some elements between minerals and melt can be very high. This can be illustrated by the example of the significant enrichment of chalcophile elements in sulfides or that of Zr and Hf in zircon.

PARTITION COEFFICIENTS OF ELEMENTS BETWEEN MINERALS AND MELT

Estimating the partition coefficients of elements between minerals and melts of various composition is one of the most important tasks in geochemistry. Experimental data on the partition of trace elements between minerals and silicate melts are periodically published (Irving, 1978; Green, 1994; Wood and Blundy, 2014). Our current dataset is continuously appended with newly acquired data, and the lists of the studied phases and elements is continuously extended. Because of this, we have analyzed publications issued before 2021 that provide data on elements discussed in Part I. A list of publications from which data were borrowed on the partition of elements is presented in the Supplementary materials.

The partition coefficients of elements ($D_i = C_i(\text{mineral})/C_i(\text{melt})$, where C_i is the weight concentration of element i) between accessory and major minerals and melts are listed in Table 1. Inasmuch as we analyze the general tendencies in the behavior of elements, the partition coefficients were evaluated using all currently available data on silicate melts at significant variations in the conditions, compositions of the melts, and concentrations of admixtures. In determining the partition coefficients of incompatible elements, one of the principal sources of the errors is the contamination of the analyses of synthetic minerals with the material of the quenched melt (glass). Because of this, a relatively small number of experiments with high concentrations of incompatible elements was discarded. To minimize the effect of contaminated analyses, the D_i values were estimated as median values. The partition coefficients of compatible elements (Ni, Cr, Co, and others) can broadly vary depending on the composition of the melt and thermodynamic parameters. We do not analyze these vari-

ations herein and have determined only median D_i values for these elements (Table 1).

Data in Table 1 show that the D_i of some elements between accessory minerals and melt can be very high (e.g., $D_{Ag, Au, Ni, Cu, Se} > 100$ for sulfide; $D_{Cr} > 100$ for spinel; $D_{Nd} > 200$ for apatite; $D_{Pr, Y} > 20$ for apatite; and $D_{Ta} > 70$ for rutile). At the same time, D_i for rock-forming minerals are usually no higher than 10 (Table 1). Because of this, the separation of even small amounts of accessory phases can notably modify ratios of elements in the residual melts. To analyze the behavior of elements at the crystallization of melt, it is convenient to analyze ratios of the concentrations of elements to the concentration of one of the most incompatible elements that is practically completely retained in melt. Among the elements analyzed herein, this is, for example, Cs. For almost all major and accessory minerals, $D_{Cs} < 0.1$, and only for biotite $D_{Cs} \sim 0.5$. Moreover, Cs was analyzed in a great number of samples (Part I), and hence, it is convenient to use this element as a reference one. A change in the concentration of element i in melt to the Cs concentration in this melt at the crystallization of a mineral can be described by the equations $(C_i/C_{Cs}) : (C_i/C_{Cs})^0 = (1 - \alpha + D_{Cs}\alpha)/(1 - \alpha + D_i\alpha)$ for equilibrium crystallization and $(C_i/C_{Cs}) : (C_i/C_{Cs})^0 = (1 - \alpha)(d_i - 1)/(1 - \alpha)(d_{Cs} - 1)$ for fractional crystallization, where C_i^0 is the concentration (in wt %) of element i in the original melt, C_i is the concentration (in wt %) in differentiated melt, and α is the weight fraction of the mineral. It is therewith assumed that the partition coefficient does not vary in the course of crystallization. This simplification is warranted and justified because the amounts of accessory minerals are insignificant. The calculated changes in the ratios of elements to Cs at the crystallization of rock-forming and accessory minerals are listed in Table 2. The calculations were conducted using the maximum amounts of accessory minerals that can crystallize from the dominant melts with average concentrations of elements critical of a given mineral (S for sulfide, Ti for rutile and ilmenite, etc.) in the melts. The difference between equilibrium and fractional crystallization is negligibly small in most instances. The ratios C_i/C_{Cs} in melts decreases notably more rapidly only for compatible elements. In spite of the high partition coefficients, the geochemical effects of the crystallization of accessory minerals are sometimes insignificant because of the low contents of these minerals. At the same time, the crystallization of a large amount of rock-forming minerals can appreciably affect the behavior of mildly compatible elements.

The discussed behaviors of the elements in crystallization processes differ (Table 2). The most incompatible elements (Ba, Be, Cl, Li, Mo, Nb, Th, U, and W) are characterized by very insignificant changes in their ratios to Cs during crystallization: $(C_i/C_{Cs}) : (C_i/C_{Cs})^0 > 0.95$. The ratios of these elements to Cs and to one another

Table 1. Partition coefficients of elements between minerals and melt: literature and experimental data

Element	Sul	Ilm	Sp	Cr-Al Sp	Mt	Ap	Bt	Rt	Zc	Oi	Opx	Cpx	Pl	Grt	Amph
Ag	265	—	—	—	—	—	—	—	—	—	—	—	—	—	—
As	10.4	—	—	—	—	—	—	—	—	—	—	—	—	—	—
Au	462	—	0.08	—	—	—	—	—	—	0.002	—	—	—	0.52	—
B	—	—	0.02	—	—	—	0.44	—	0.002	0.036	0.06	0.06	0.15	0.02	1
Ba	—	0.002	0.0006	0.0006	—	0.082	2.1	0.04	0.1	0.00016	0.00077	0.00098	0.23	0.006	0.12
Be	—	—	0.09	0.09	—	0.89	0.42	0.05	0.11	0.0024	0.061	0.17	0.25	0.086	0.17
Bi	132	—	—	—	—	—	—	—	—	—	—	—	—	0.04	—
Br	0.3	—	—	—	—	—	—	—	—	—	—	—	—	—	—
Cd	29.2	—	—	—	—	—	3.1	—	—	—	—	—	1.3	0.88	—
Ce	0.025	0.001	0.007	0.043	0.004	19.2	0.016	0.0022	0.27	0.00016	0.0029	0.074	0.049	0.013	0.34
Cl	0.18	—	0.25	—	0.09	3	0.74	—	—	0.011	0.0066	0.064	0.0015	0.041	0.29
Co	47.3	2.2	5.5	4.2	9.4	14.2	6.2	0.03	0.25	1.9	1.5	1	0.036	1.5	3.4
Cr	2.9	9.9	172	198	27	1	3.4	15	0.7	0.75	2.9	5.7	0.45	6.2	4.3
Cs	0.033	—	0.034	0.034	—	0.00017	0.57	0.12	0.07	0.00087	0.01	0.0035	0.0027	0.0053	0.0025
Cu	473	1.4	0.56	0.23	0.82	5.4	1.1	0.8	0.43	0.078	0.11	0.1	0.09	0.065	0.078
F	—	—	0.05	—	0.12	11.6	3	—	—	0.0025	0.03	0.046	0.1	0.0082	1.4
Ga	0.079	0.3	3.1	4.4	1.1	0.78	1.2	0.1	0.1	0.022	0.23	0.35	0.86	0.41	0.7
Ge	0.73	—	0.26	0.26	—	—	—	—	—	0.47	0.95	0.98	0.5	0.76	—
I	1.1	—	—	—	—	—	1	—	—	—	—	—	—	—	—
In	7.7	—	3.3	—	3.3	—	5.1	—	—	0.095	—	0.48	0.078	1	35
La	0.05	0.002	0.005	0.029	0.0037	4.9	0.016	0.0055	0.63	0.00065	0.0014	0.06	0.076	0.0068	0.18
Li	0.061	—	0.1	0.1	—	0.52	0.46	0.06	0.1	0.19	0.22	0.29	0.2	0.16	0.17
Mo	12	1.7	0.03	0.032	0.03	—	—	—	—	0.011	0.02	0.015	0.01	0.1	0.024
Nb	0.018	0.7	0.033	0.0006	0.066	0.0018	0.075	6.5	0.63	0.00012	0.0015	0.0054	0.002	0.013	0.45
Nd	0.14	0.0008	0.01	0.05	0.01	230	0.025	0.04	1.4	0.00005	0.007	0.15	0.04	0.06	0.79

Table 1. (Contd.)

Element	<i>Sul</i>	<i>Ilm</i>	<i>Sp</i>	<i>Cr-Al Sp</i>	<i>Mt</i>	<i>Ap</i>	<i>Bt</i>	<i>Rt</i>	<i>Zc</i>	<i>Ol</i>	<i>Opx</i>	<i>Cpx</i>	<i>Pl</i>	<i>Grt</i>	<i>Amph</i>
Ni	413	4	8	6.3	17	12.9	9.7	0.6	0.9	5.4	2.4	2	0.54	0.6	4
Pb	18	—	—	—	—	0.49	0.12	1.5	0.16	0.0012	0.005	0.03	0.24	0.0089	0.069
Pr	0.05	0.0004	0.007	0.03	0.006	22	0.024	0.003	1	0.00003	0.004	0.08	0.06	0.02	0.56
Rb	0.026	—	0.008	0.0078	—	0.0009	2	0.01	0.11	0.0014	0.003	0.0068	0.022	0.0088	0.037
S	124	—	—	—	—	5.6	—	—	—	0.0044	0.024	0.13	—	—	0.9
Sb	12.5	0.05	—	—	—	—	—	1.2	—	0.016	0.18	1.1	—	—	—
Sc	—	0.83	0.6	0.056	1.4	4.8	0.23	0.31	37	0.16	0.6	1.8	0.035	3.7	9.2
Se	107	—	—	—	—	—	—	—	—	—	—	—	—	—	—
Sm	0.15	0.003	0.032	0.11	0.015	10	0.04	0.003	1.8	0.0003	0.018	0.32	0.03	0.3	1.2
Sn	5.4	5	—	—	—	—	—	—	—	—	0.9	3.3	0.11	0.11	6.1
Sr	—	0.003	0.05	0.036	0.13	4.4	0.18	0.012	0.049	0.00065	0.0034	0.092	1.6	0.01	0.33
Ta	0.003	1	0.07	0.0004	0.12	0.0016	0.05	76	3.5	0.000051	0.0011	0.0095	0.001	0.019	0.34
Th	0.0036	0.0007	0.003	0.00013	0.006	0.96	0.012	0.0011	8.4	4.00E-06	0.0011	0.0046	0.00058	0.019	0.021
Tl	6.7	—	—	—	—	—	—	—	—	—	—	—	—	0.09	—
U	0.03	0.005	0.0001	0.00014	0.0001	0.53	0.032	0.41	16.5	6.00E-06	0.0014	0.0035	0.0013	0.038	0.016
V	0.29	5.5	2.3	3.8	0.67	18.4	3.9	6.1	0.9	0.125	0.71	1.9	0.025	2.2	4.1
W	0.05	0.057	0.0002	0.00015	0.00025	—	—	5.3	—	0.000073	0.0013	0.00027	0.00011	0.05	0.021
Y	—	0.015	0.007	0.0012	0.021	32	0.017	0.031	24	0.0067	0.045	0.35	0.0095	2.6	1.65
Zn	1.2	0.95	6.9	6.9	7	4.7	1.4	9.3	—	1.1	0.69	0.54	0.13	0.81	3
Zr	0.005	0.33	0.04	0.0012	0.055	0.041	0.018	7.8	117	0.0007	0.0066	0.1	0.0025	0.3	0.76

The table presents median values of data published on each element. Values printed in italics are based on small numbers (1–4) of analyses or those with very broad variations (e.g., from 100 to 0.01). Mineral symbols: *Sul*—sulfide (crystalline and melt); *Ilm*—ilmenite; *Sp*—spinel (including magnetite and titanomagnetite); *Mt*—magnetite and titanomagnetite; *Ap*—apatite; *Bt*—biotite; *Rt*—rutile; *Zc*—zircon; *Ol*—olivine; *Opx*—1 opx; *Cpx*—1 cpx; *Pl*—plagioclase; *Grt*—garnet; *Amph*—monoclinic amphibole. See the Supplementary for references to experimental data.

Table 2. Model changes in C_i/C_{Cs} (wt %) at the crystallization of minerals from starting melt with $C_i^0/C_{Cs}^0 = 1$

Element	<i>Sul</i>	<i>Ilm</i>	<i>Sp</i>	<i>Cr-Al Sp</i>	<i>Mt</i>	<i>Ap</i>	<i>Bt</i>	<i>Rt</i>	<i>Zc</i>	<i>Oi</i>	<i>Opx</i>	<i>Cpx</i>	<i>Pl</i>	<i>Grt</i>	<i>Amph</i>
α	0.0033	0.04	0.01	0.001	0.01	0.01	0.04	0.01	0.00025	0.1	0.1	0.1	0.1	0.1	0.1
Ag	0.53–0.42	–	–	–	–	–	–	–	–	–	–	–	–	–	–
As	0.97	–	–	–	–	–	–	–	–	–	–	–	–	–	–
Au	0.4–0.22	–	1	–	–	–	–	–	–	1	–	–	–	0.95	–
B	–	–	1	1	–	–	1	–	1	1	0.99	0.99	0.98	1	0.9
Ba	–	1	1	1	–	1	0.94	1	1	1	1	1	0.98	1	0.99
Be	–	–	1	1	–	0.99	1	1	1	1	0.99	0.98	0.97	0.99	0.98
Bi	0.70–0.65	–	–	–	–	–	–	–	–	–	–	–	–	1	–
Br	1	–	–	–	–	–	–	–	–	–	–	–	–	–	–
Cd	0.91	–	–	–	–	–	0.9	–	–	–	–	–	0.87	0.91	–
Ce	1	1	1	1	1	0.84–0.82	1.02	1	1	1	1	0.99	0.99	1	0.96
Cl	1	–	1	–	1	0.97	0.99	–	–	1	1	0.99	1	1	0.97
Co	0.86	0.92	0.95	1	0.91	0.87	0.81–0.79	1	1	0.82	0.85	0.9	1	0.85	0.72–0.7
Cr	0.99	0.71–0.67	0.37–0.18	0.83	0.79–0.76	0.99	0.89	0.87–0.86	1	0.92	0.76–0.74	0.61–0.55	0.95	0.59–0.52	0.68–0.64
Cu	0.39–0.21	0.94	0.99	1	0.99	0.95	0.98	0.99	1	0.99	0.99	0.99	0.99	0.99	0.99
F	–	–	1	–	1	0.89	0.91	–	–	1	1	1	0.99	1	0.87–0.86
Ga	1	0.99	0.97	1	0.99	0.99	0.98	1	1	1	0.98	0.96	0.91	0.96	0.93
Ge	1	–	1	1	–	–	–	–	–	0.95	0.91	0.9	0.95	0.92	–
I	1	–	–	–	–	–	0.98	–	–	–	–	–	–	–	–
In	0.98	–	0.97	–	0.97	–	0.84–0.83	–	–	0.99	–	0.95	0.99	0.9	0.21–0.03
La	1	1	1	1	1	0.95	1.02	1	1	1	1	0.99	0.99	1	0.98
Li	1	–	1	1	–	0.99	1	1	1	0.98	0.98	0.97	0.98	0.98	0.98
Mo	0.96	0.93	1	1	1	–	–	–	–	1	1	1	1	0.99	1

Table 2. (Contd.)

Element	<i>Sul</i>	<i>Ilm</i>	<i>Sp</i>	<i>Cr-Al Sp</i>	<i>Mt</i>	<i>Ap</i>	<i>Bt</i>	<i>Rt</i>	<i>Zc</i>	<i>OI</i>	<i>Opx</i>	<i>Cpx</i>	<i>Pl</i>	<i>Grt</i>	<i>Amph</i>
Nb	1	0.97	1	1	1	1	1.02	0.94	1	1	1	1	1	1	0.95
Nd	1	1	1	1	1	0.1–0.3	1.02	1	1	1	1	0.98	1	0.99	0.92
Ni	0.42–0.26	0.85	0.92	0.99	0.85–0.84	0.88	0.73–0.69	1	1	0.62–0.56	0.79–0.78	0.82–0.81	0.94	0.94	0.69–0.66
Pb	0.94	–	–	–	–	1	1.02	0.99	1	1	1	1	0.97	1	0.99
Rb	1	–	1	1	–	1	0.94	1	1	1	1	1	1	1	1
S	0.71–0.66	–	–	–	–	0.95	–	–	–	1	1	0.99	–	–	0.91
Sb	0.96	1	–	–	–	–	–	0.99	–	1	0.98	0.89	–	–	–
Se	0.70–0.73	–	–	–	–	–	–	–	–	–	–	–	–	–	–
Sm	1	1	1	1	1	0.9	1.02	1	1	1	1	0.97	1	0.97	0.87
Sc	–	0.97	0.99	1	0.99	0.95	1.01	1	0.99	0.98	0.94	0.83	1	0.71–0.68	0.50–0.38
Sn	0.98	0.83–0.81	–	–	–	–	–	–	–	–	0.91	0.73–0.71	0.99	0.99	0.60–0.52
Sr	–	1	1	1	1	0.96	1.02	1	1	1	1	0.99	0.85	1	0.97
Ta	1	0.96	1	1	1	1	1.02	0.57–0.47	1	1	1	1	1	1	0.96
Th	1	1	1	1	1	0.99	1.02	1	1	1	1	1	1	1	1
Tl	0.98	–	–	–	–	–	–	–	–	–	–	–	–	0.99	–
U	1	1	1	1	1	0.99	1.02	1	1	1	1	1	1	1	1
V	1	0.81–0.80	0.98	1	0.99	0.84–0.83	0.88	0.94	1	0.99	0.93	0.82	1	0.80–0.79	0.69–0.65
W	1	1	1	1	1	–	–	0.95	1	1	1	1	1	0.99	1
Y	–	1	1	1	1	0.76–0.73	1.02	1	0.99	1	1	0.96	1	0.78–0.76	0.84
Zn	1	0.96	0.93	0.99	0.93	0.95	0.97	0.91	–	0.89	0.93	0.94	0.99	0.92	0.75–0.73
Zr	1	0.99	1	1	1	1	1.02	0.93	0.97	1	1	0.99	1	0.97	0.92

The mass fraction of crystallizing mineral (α) is calculated from the concentrations of critical elements in the average melt compositions (Zr for zircon, Ti for rutile, etc.). For rock-forming minerals, we assumed $\alpha = 0.1$. Equilibrium and fractional crystallization result in practically equal values in most situation. At high D values, fractional crystallization can sometimes result in much lower ratios than those at equilibrium crystallization. In this situation, ranges from the maximum to minimum values (for equilibrium and fractional crystallization, respectively) are reported.

should most correspond to the source of the melts if the residual melt does not retain much accessory minerals. There are elements whose ratios to Cs can significantly vary only at the crystallization of a certain mineral, whereas the effects of other minerals are negligibly small. This means that the ratios of these elements to Cs (or another incompatible element) is an indicator of the crystallization of only a single particular accessory or rock-forming mineral. These elements are Ce and Nd for apatite, Cu for sulfide, Sr for plagioclase, and Ta for rutile. Finally, some elements are mildly or strongly compatible to a few minerals, either rock-forming or accessory. The relative concentrations of these elements (Co, Cr, In, Ni, Sc, V, and Y) most significantly vary in the course of crystallization. For example, the Ni/Cs ratio notably decreases at the crystallization of even small amounts of sulfide, and the crystallization of much olivine and pyroxenes results in a comparable effect. Cobalt is accommodated in noticeable concentrations in practically all of the minerals. The behavior of Y and Sc is controlled by two minerals: garnet and amphibole. In addition, the crystallization of pyroxenes can significantly decrease the Sc/Cs ratio, and the crystallization of apatite affects the Y/Cs ratio.

VARIATIONS IN RATIOS OF ELEMENTS IN MELTS

Differences in the behavior of elements are reflected in the covariations in the ratios of elements to Cs (Figs. 1–4).

Two other most incompatible elements, along with Cs, are Ba and La. Because of this, the Ba/Cs and La/Cs ratios should reflect the composition of the source and not vary in the course of crystallization differentiation. In this situation, possible correlations in the Ba/Cs–La/Cs diagram should pass through zero. The diagram in Fig. 1 shows significant variations in both ratios. For environment I (mid-oceanic ridges), significant variations are typical of the La/Cs ratio, which does not correlate with the Ba/Cs ratio. This seems to reflect variations in the compositions of the sources from Ba/La ~ 12 , which is fairly close to the value typical of the primitive mantle (~ 10 ; Palme and O'Neill, 2014), to Ba/La ~ 2 , which is much lower than is hypothetically typical of the depleted mantle (~ 5.1 ; Salters and Stracke, 2004). The likely reason for the slight shift in the compositions may be the crystallization of apatite and biotite, although these effects are much smaller than the actual variations (Fig. 1).

The La/Cs ratio of mafic melts in environment II (oceanic islands) varies much less significantly and obviously correlates with the Ba/Cs ratio (Fig. 1). This correlation is not related to crystallization differentiation and corresponds to a constant Ba/La ratio that is close to that in the primitive mantle (~ 10). A less obvious trend is discernible toward the composition of the depleted mantle source (DM). At the same time, the

compositions of felsic melts notably deviate from this correlation and are characterized by a roughly constant La/Cs ~ 80 . This may be explained by a significant fraction of biotite during the crystallization of intermediate and felsic melts and/or the effect of fluid-assisted transport and contamination.

Environments III (island arcs) and IV (active continental margins) are characterized by low La/Cs ratios and significant variations in Ba/Cs (Fig. 1). The Ba/La ratios are usually higher than 20, and there are obviously some sources in which this ratio is different. The effect of crystallization differentiation is insignificant, and the fields of mafic and felsic rocks almost exactly coincide.

The mafic melts of environment V (continental rifts and hotspots) are also characterized by high Ba/La ratios, but the felsic melts (which are dominant in this environment) define a number of trends with much lower Ba/La ratios, up to ~ 2 .

The mafic melts of environment VI (backarc basins) exhibit significant and unsystematic variations in the Ba/La ratio, which are comparable to those in environment I (although the numbers of the measurements is much lower) (Fig. 1).

Another example of variations in concentrations of components that are controlled primarily by the composition of the source is offered by Th/Cs–Nb/Cs diagrams (Fig. 2). In these diagrams, the fractionation effects of major and minor minerals are negligibly small. For environment I, the correlation is strong at Nb/Th ~ 15 , which is close to the evaluated composition of the depleted mantle (Salters and Stracke, 2004). The average Th/Cs and Nb/Cs ratios are also close to those of DM but show broad variations. The contributions of sources compositionally similar to the primitive mantle (PM) or continental crust (CC) are insignificant in this instance. At the transition to environment II, the variations in the Nb/Th ratio remarkably diminish, and another source, in addition to DM (Nb/Th ~ 15), is discernible, which has much lower Nb/Th ratios, close to those assumed for the primitive mantle (7; Palme and O'Neill, 2014). All transitional compositions are also found, which may indicate a mixed source with variable proportions of the DM and PM materials.

For the rest of the environments (III–VI), the determining factors is the contributions of sources whose Nb/Th ratios are close to those of the continental crust (1.4; Rudnick and Gao, 2014). The most homogeneous composition is typical of the source of environments III and IV, whereas the melts of environments V and VI provide evidence of the involvement of material similar to DM and, perhaps, also to PM (Fig. 2).

Principally different relationships are displayed in diagrams for elements susceptible to crystallization processes, for example, Cu/Cs–Ta/Cs (Fig. 3). The former ratio varies at the separation of sulfide melt or

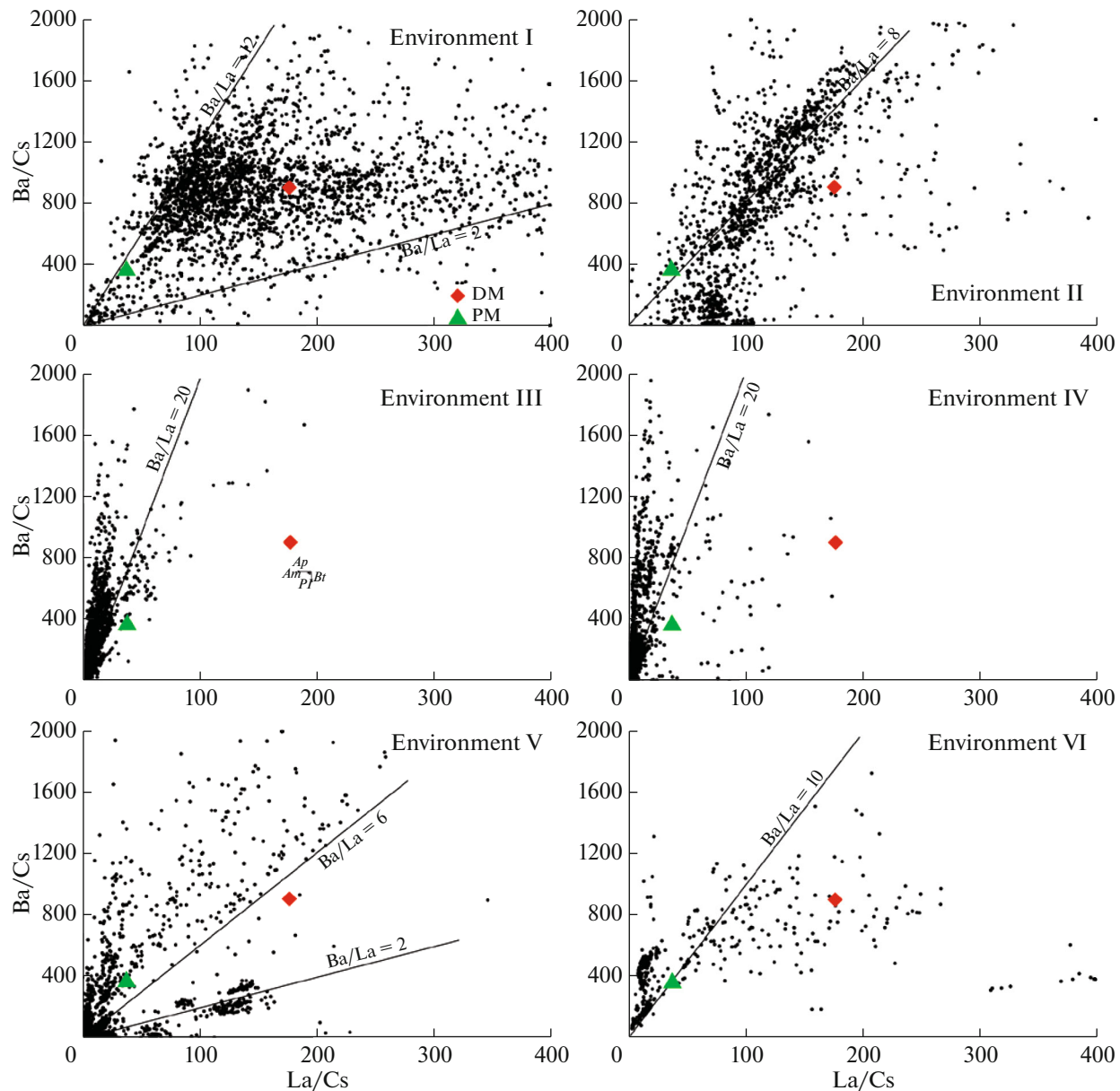


Fig. 1. Covariations in the La/Cs–Ba/Cs ratios of melt inclusions and glasses of rocks of the dominant geodynamic environments. The diagrams also show the compositions of the primitive mantle (PM, according to Palme and O’Neill, 2014), depleted mantle (DM, according to Salters and Stracke, 2004), and continental crust (CC, according to Rudnick and Gao, 2014). Arrows show how the ratios vary at the crystallization of specified amounts of rock-forming and accessory minerals from melt: 10 wt % amphibole (*Am*), 1 wt % apatite (*Ap*), 4 wt % biotite (*Bt*), 10 wt % garnet (*Grt*), 4 wt % ilmenite (*Ilm*), 10 wt % clinopyroxene (*Cpx*), 10 wt % olivine (*Ol*), 10 wt % orthopyroxene (*Opx*), 10 wt % plagioclase (*Pl*), 1 wt % rutile (*Rt*), and 0.33 wt % sulfide (*Sul*). Only minerals that can appreciably modify at least a single ratio are shown.

the crystallization of sulfides, and the latter one is susceptible to rutile crystallization. None of these ratios is susceptible to the removal or addition of any other accessory or rock-forming minerals. For environment I, wide and unsystematic variations are shown by both ratios, with Cu/Ta varying from values corresponding to DM (~2200; Salters and Stracke, 2004) to those much lower than Cu/Ta = 465, which is typical of the primitive mantle (Palme and O’Neill,

2014). The absence of correlations between the Cu/Cs and Ta/Cs ratios indicates that the scatters in their values were caused by an independent process. As follows from calculations (Fig. 3), the separation of even small amounts of rutile and sulfides almost twofold decreases the Ta/Cs and Cu/Cs ratios (Table 2), and hence, the variations could be caused by these minerals.

For environment II, the effects of sulfide accumulation is insignificant, because almost none of the

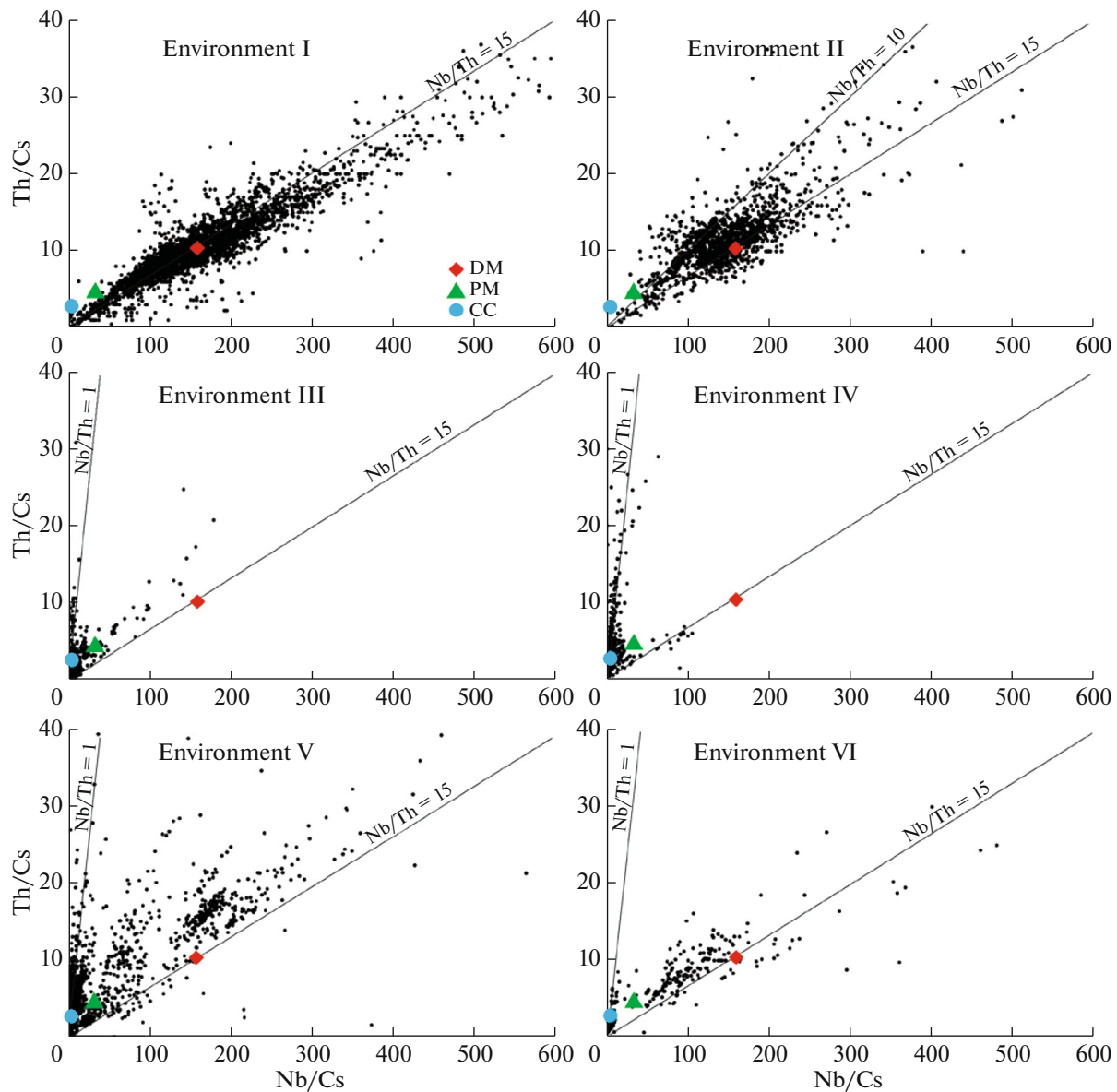


Fig. 2. Covariations in the Nb/Cs–Th/Cs ratios in melt inclusions and glasses of rocks of the dominant geodynamic environments. See Fig. 1 for symbol explanations.

melts possesses high Cu/Cs ratios. Most of the compositions have Cu/Ta ratios lower than in the primitive mantle. Very low Cu/Ta ratios (<200) can result from the separation of sulfides. For environments III–V, the Cu/Cs ratio is low and the Ta/Cs ratios significantly varies, which suggests that rutile may have played a significant role in the evolution of these magmas. The variations in the compositions of environment VI resemble what was seen in environment I, at a much lower amount of the data. The relatively definitely discernible trend parallel to the Cu/Cs axis seems to reflect the effect of sulfides on the composition of the silicate melt.

It is interesting to analyze the behavior of elements whose concentrations in rock-forming minerals are

high. As an example, Fig. 4 presents V/Cs–Co/Cs diagrams. Both V and Co are elements moderately compatible with pyroxene, garnet, biotite, and amphibole; Co is also compatible with olivine and sulfides, whereas V is compatible with ilmenite. However, effects related to the crystallization of these phases are less significant than the aforementioned effects of sulfides and rutile on the behavior of Cu and Ta, respectively. As a result, in spite of variations in the Co/Cs and V/Cs ratios during the crystallization of melts, these ratios show a stable correlation (Fig. 4). As in the instances discussed above, the maximal variations occur in environment I, which may be partly explained by the large volume of the data. Therewith the V/Ca ratios are most often much higher than those of the

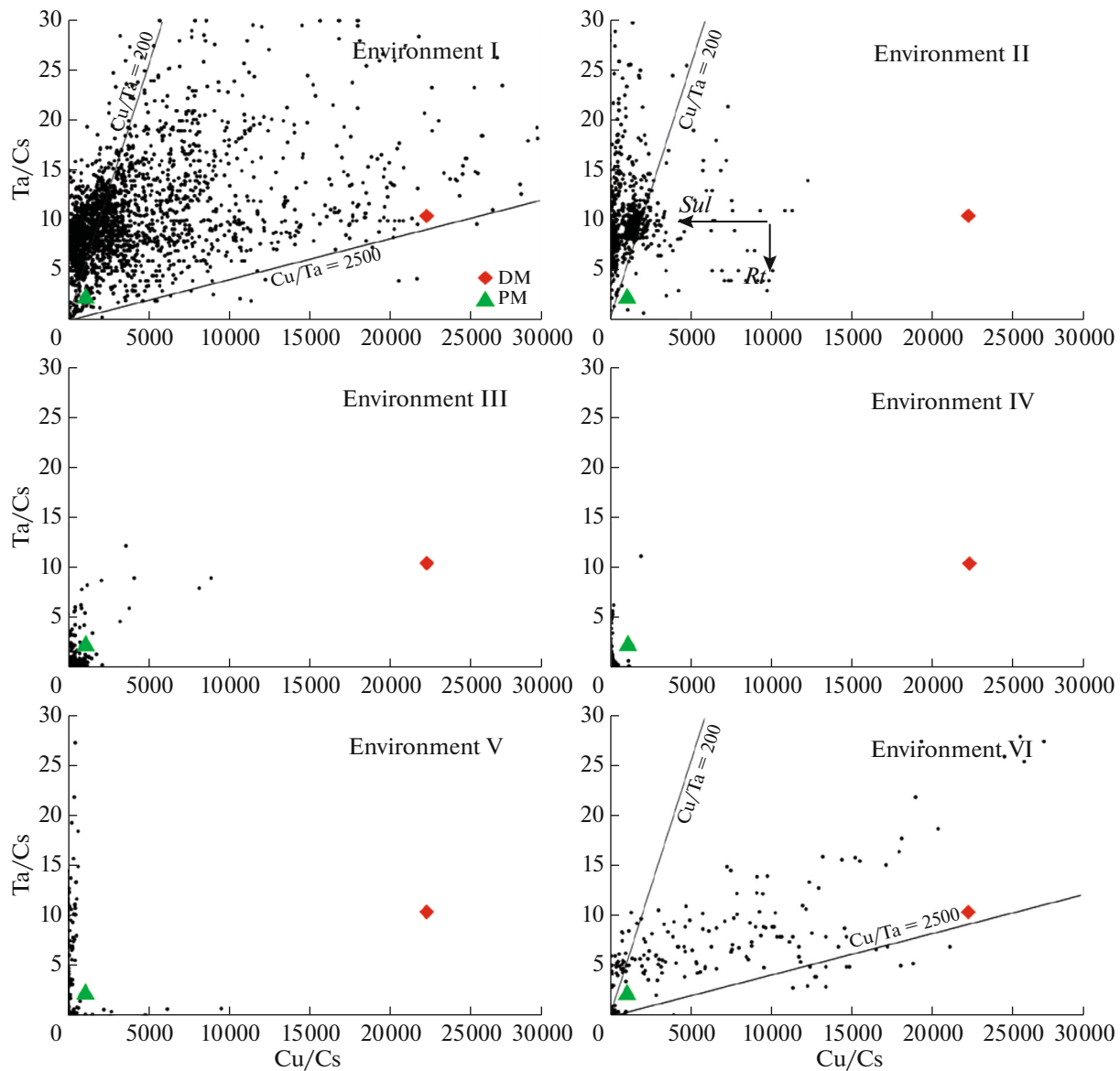


Fig. 3. Covariations in the Cu/Cs–Ta/Cs ratios in melt inclusions and glasses of rocks of the dominant geodynamic environments. See Fig. 1 for symbol explanations.

primitive mantle (~ 0.85 ; Palme and O'Neill, 2014) and depleted one (0.75; Salters and Stracke, 2004). The likely reason for this is the stronger compatibility of Co with olivine and orthopyroxene, the dominant minerals of mantle residues. A certain contribution can also be made by the decrease in the Co/Cs ratio at the separation of sulfides.

It is also worth mentioning that the composition fields of melts in the V/Cs–Co/Cs diagram almost fully overlap one another (Fig. 4), which is quite unexpected with regard to the very different compatibilities of these elements. This systematic arrangement of the compositions may perhaps be explained by small variations in the V/Co ratio in the sources, which is consistent with the similar V/Co ratios in the primitive

and depleted mantle. At the same time, this also provides evidence that the magmas were derived and then crystallized under similar conditions, because the V/Cs and Co/Cs ratios change if major rock-forming silicates are added or removed.

Our analysis enabled us to distinguish a group of the most incompatible elements, whose ratios in melts provide insights into the compositions of the magma sources and are not modified when major and accessory minerals crystallize. These elements are Ba, Be, Cs, La, Li, Th, U, and W. The specific behavior of some elements can be controlled by the fractionation of an accessory or rock-forming mineral. Variations in the ratios of such elements to the most incompatible ones are in this situation sensitive indicators of the

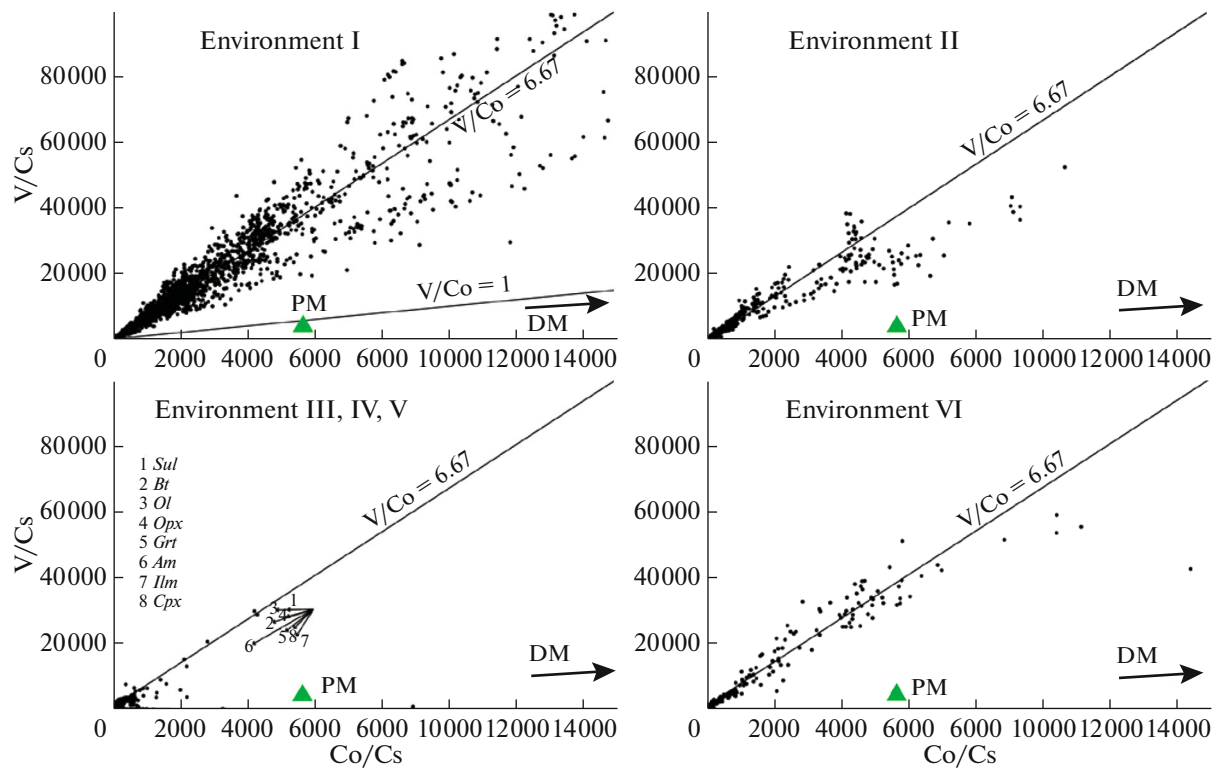


Fig. 4. Covariations in the Co/Cs–V/Cs ratios in melt inclusions and glasses of rocks of the dominant geodynamic environments. See Fig. 1 for symbol explanations.

removal or assimilation of corresponding minerals. Such indicator elements are Cu for sulfides, Ce and Nd for apatite, Nb and Ta for rutile, Sr for plagioclase, and In for amphibole. Rutile crystallization not only decreases Ta and Nb concentrations in residual melts but also leads to the effective fractionation of these elements. The removal of as little as 1 wt % rutile 1.6–2 times decreases the Ta/Nb ratio (Table 1). The relative concentrations of many elements can be significantly changed at the crystallization of several phases, either accessory or rock-forming. These compatible or weakly incompatible elements are Co, Cr, Ni, Sc, Sn, V, Y, and Zn. Interpretations of variations of the ratios of such elements to incompatible elements is a challenging problem, which requires an individual approach in each particular instance.

The diagrams of ratios of various elements to Cs presented in Figs. 1–4 show that the widest variations in the ratios of incompatible elements are typical of melts in mid-oceanic ridges (environment I). These ratios reflect the composition of the melt sources, which makes it possible to conclude that the sources of basalt melts in mid-oceanic ridges vary in composition from the DM model composition to those of the primitive mantle and even more enriched materials. Such significant variations in the composition of the sources of environment I may be explained by that this envi-

ronment is characterized by the most extensive melting of the mantle, a processes that involves volumes greater than the characteristic sizes of mantle heterogeneities. In the other environments, magmas are derived more locally, and hence melting is selective and mostly involves zones of low-melting rocks. These differences may be also partly explained by that environment I is represented by the largest dataset. However, lately much data were also accumulated on the other environments (see Part I), but the differences between the ratios of incompatible elements still remain significant.

SIMILARITIES AND DIFFERENCES BETWEEN MELTS IN VARIOUS GEODYNAMIC ENVIRONMENTS

Figure 5 shows average concentrations of elements in melts in various geodynamic environments (Part I) normalized to the composition of the primitive mantle (Palme and O'Neill, 2014). Elements are arranged in this diagram in ascending order of their bulk partition coefficients between mantle material, which was assumed to consist of 0.59 olivine + 0.15 orthopyroxene + 0.10 clinopyroxene + 0.05 plagioclase + 0.10 garnet + 0.01 spinel. Of course, this mineral association does not correspond to any real peridotite, but the average compositions of melts do not also correspond

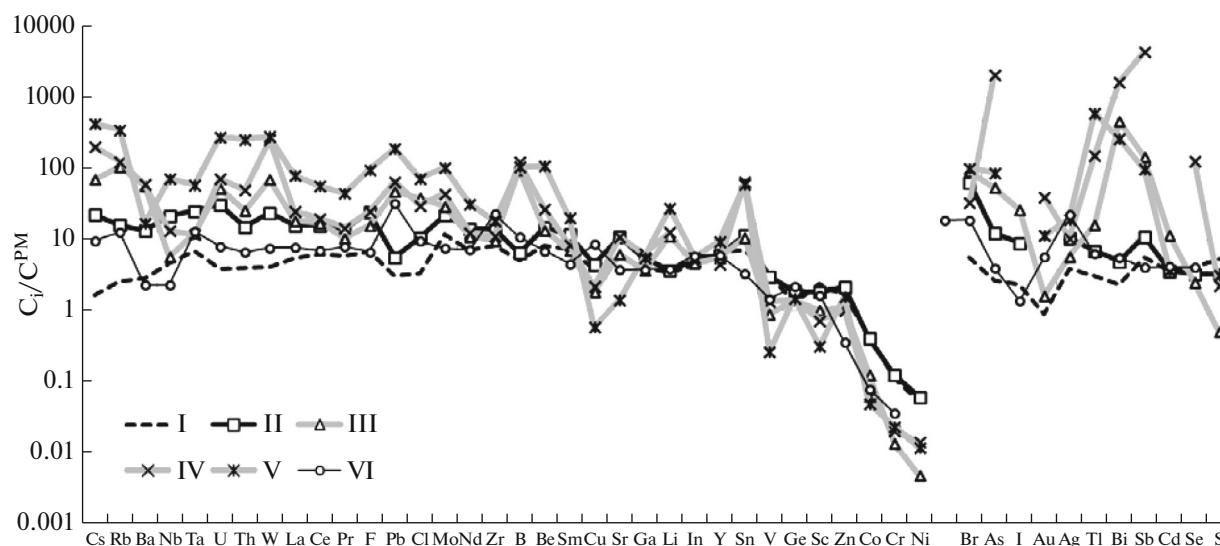


Fig. 5. Primitive mantle-normalized (Palme and O'Neill, 2014) patterns of average concentrations of elements in melts from various geodynamic environments (I–VI). Elements from Cs through Ni are arranged in ascending order of their bulk partition coefficients between model mantle material and melt, calculated from averaged published experimental data. For elements in the right-hand part of the diagram (from Br through S), experimental data are either absent or too fragmentary.

to the composition of any given magma but are an integral characteristic of melts derived under different conditions and then variably fractionated. The order of elements in the leftmost part of the diagram is slightly modified to combine geochemically similar pairs: U–Th and Nb–Ta. Elements on which no reliable experimental data are available for the aforementioned phases are shown in the right-hand part of the diagram. These are mostly volatile and chalcophile elements (Fig. 5, from Br through S).

Figure 5 displays significant variations in concentrations of elements in melts from various geodynamic environments, with these variations being the greatest for the most incompatible elements. It is clearly seen that the melts of mid-oceanic ridges (environment I) are depleted, and the melts of marginal and continental environments (environments III–V) are enriched. To make the differences between the compositions even more obvious, we used, again, ratios of the concentrations of the elements to that of Cs and then normalized them to the ratios in the average compositions of melt from environment I (Fig. 6). In this diagram, melts from environment I plot on a straight line sloped at 1. Most elements from the other environments plot below this line, which reflects, first of all, low Cs concentrations in the melts of mid-oceanic ridges. At the same time, most elements show a systematic distribution in the diagram.

Normalized concentrations of elements in the melts of oceanic islands (environment II) gradually decrease from the most incompatible elements to compatible ones. All deviations from this trend are within the corresponding analytical inaccuracies. This systematic distribution may be explained by geochem-

ical similarities between the sources of melts in environments I and II at lower degrees of melting in environment II (McKenzie and O'Nions, 1991).

The melts of continental and continental-marginal environments (III–V) generally show an analogous trend but much lower normalized elemental ratios and a number of anomalies. One of them is the well-known Ta–Nb minimum, which is seen in most marginal environments (Briqueu et al., 1984) and is likely explained by that rutile is involved in magma derivation and evolution (Kelemen and Hanghøj, 2003) or by the effect of fluid-assisted transfer of elements (Baier et al., 2008). Enrichment in Pb is one of the characteristics of suprasubductional environments and continental crust (Pearce and Peate, 1995; Hofmann, 1988; Rudnick and Gao, 2014). Evidence of this is provided by melts in all continental and marginal environments. Other anomalies of these environments (which are clearly seen in Fig. 5) are that the melts are relatively enriched in W, B, Li, and Sn. Interpretations of these anomalies are ambiguous. It is quite probable that a noticeable role is therewith played by fluid, at least in what concerns B (Ryan and Langmuir, 1993). Melts in backarc basins (environment VI) are transitional: concentrations of most elements in them are practically exactly identical to those in the melts of oceanic islands (environment II), but the former show clearly discernible Nb–Ta minima. This is likely explained by unusual conditions under which magmas are generated beneath backarc basins and which stabilize rutile in the mantle material and/or intermediate magma chambers.

The distribution of volatile and chalcophile elements in the right-hand part of the diagram (Figs. 5, 6)

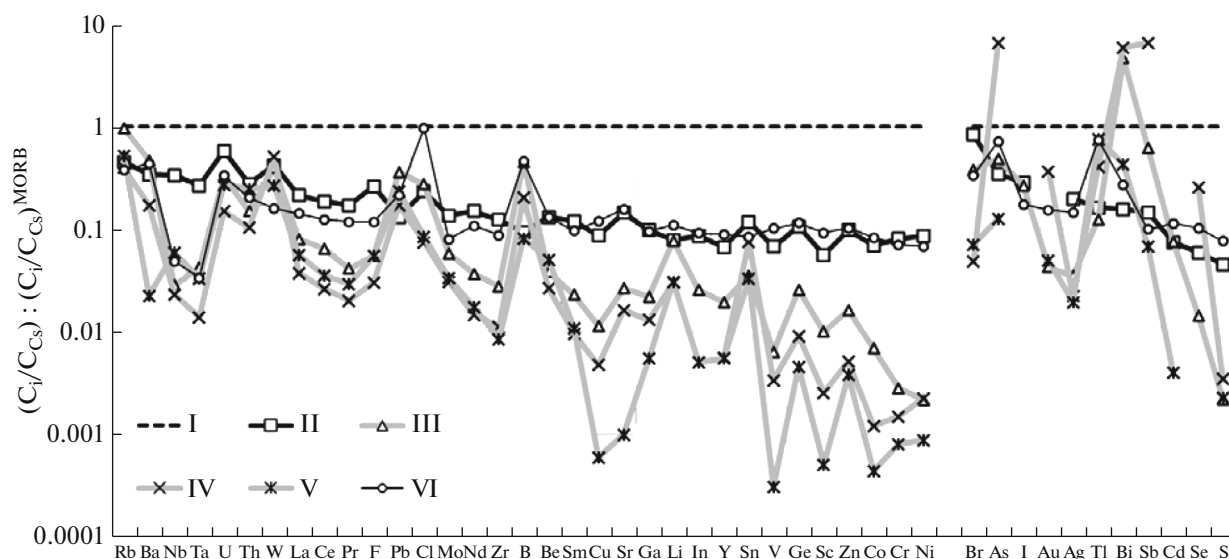


Fig. 6. Ratios of concentrations of elements to that of Cs in the average composition of melts from geodynamic environments I–IV normalized to the average composition of melts in mid-oceanic ridges (environment I).

led us to suggest how these element may behave in magma-generating processes. To do this, we arranged these elements in descending order of their ratios to Cs in the average composition of environment II (Figs. 5, 6). This enabled us to compare elements for which no reliable experimental data are available with other elements from the main succession in Figs. 5, 6. The volatile elements (Br, As, and I) are obviously comparable with the most incompatible elements (Rb, Ba, and others). The moderately chalcophile and moderately volatile elements Bi, Sb, and Cd are comparable with incompatible elements in the middle parts of the patterns in Figs. 5 and 6, for example, with MREE and Zr, and this does not contradict currently available fragmentary experimental data. It is interesting that the S/Cs and Se/Cs ratios are low and comparable to the ratios of more compatible elements, such as V, Sc, and Zn. This behavior of S and Se is indicative of that that magma generation and crystallizing regions may contain sulfides. However, it is worth mentioning that the behavior of Au and Ag is more incompatible than that of S, although the average experimentally determined partition coefficients of Ag and Au between sulfide and melt are much higher than the partition coefficient of S (Table 1). It can be hypothesized that the experimental values presented for Au and Ag are significantly overestimated because of the contamination of the sulfides with a metal phase. If so, the minimum values of the partition coefficients may be more accurate. It is reasonable to suggest that the partition coefficient of Ag and Au are likely no higher than 100 (Li and Audetat, 2012, 2013, 2015), and these elements are indeed more incompatible than S (and Se) at mantle melting in the presence of sulfides.

CONCLUSIONS

In Part I, we have evaluated the average concentrations of elements in the melts of dominant geodynamic environments and listed the inherent features of these environments and the broad variations in concentrations of elements in some of the environments (these variations are characterized by standard deviations, which are listed in tables in Part I). This publication presents more detailed information on the variations in the concentrations of selected compatible and incompatible elements, and the diagrams (Figs. 1–4) demonstrate that elemental ratios broadly vary within each environment. Crystallization differentiation is one of the leading processes that control the major-element composition of melts. Comparative analysis of natural and experimental data shows that the effects of crystallization differentiation on ratios of elements are much smaller than the variations in these ratios found in melt inclusions and glasses in rocks. Considered collectively, data on the composition of natural glasses indicate that the sources of natural melts are heterogeneous. This heterogeneity also follows from geochemical and isotope data on rocks (Hofmann, 2003; Stracke, 2012). Data on the composition of inclusions and glasses make it possible to estimate how much heterogeneous are melts entrapped during various evolutionary stages of magmatic systems. Some researchers mentioned that the composition of melt inclusions varies much more significantly that the composition of the rocks (Sobolev and Shimizu, 1993; Gurenko and Chaussidon, 1995; MacLennan, 2008; Jackson et al., 2015). This indicates that melt inclusions can preserve information on the small-scale heterogeneity of the sources and variations in the conditions under

which melts are derived. This information is lost when the melts mix because of the small volumes of the melt portions coming to shallow-depth magma reservoirs. In this context, it would be interesting to compare in detail the composition of rocks and melt inclusions.

FUNDING

This study was carried out under government-financed research projects for Vernadsky Institute of Geochemistry and Analytical Chemistry, Russian Academy of Sciences (0137-2019-0016) and for Institute of Geology of Ore Deposits, Petrography, Mineralogy, and Geochemistry, Russian Academy of Sciences. The study was also partly supported by the Russian Foundation for Basic Research, project no. 19-05-00476.

CONFLICT OF INTEREST

The authors declare that they have no conflicts of interest.

SUPPLEMENTARY INFORMATION

The online version contains supplementary material available at <https://doi.org/10.1134/S0016702922060040>.

REFERENCES

- J. Baier, A. Audetat, and H. Keppler, “The origin of the negative niobium tantalum anomaly in subduction zone magmas,” *Earth Planet. Sci. Lett.* **267**, 290–300 (2008).
- L. Briquieu, H. Bougault, and J. L. Joron, “Quantification of Nb, Ta, Ti and V anomalies in magmas associated with subduction zones: petrogenetic implications,” *Earth Planet. Sci. Lett.* **68**, 297–308 (1984).
- T. H. Green, “Experimental studies of trace-element partitioning applicable to igneous petrogenesis—Sedona 16 years later,” *Chem. Geol.* **117**, 1–36 (1994).
- A. A. Gurenko and M. Chaussidon, “Enriched and depleted primitive melts included in olivine from Icelandic tholeiites: origin by continuous melting of a single mantle column,” *Geochim. Cosmochim. Acta* **59**, 2905–2917 (1995).
- A. W. Hofmann, “Chemical differentiation of the Earth: the relationship between mantle, continental crust, and oceanic crust,” *Earth Planet. Sci. Lett.* **90**, 297–314 (1988).
- A. W. Hofmann, “Sampling mantle heterogeneity through oceanic basalts: Isotopes and trace elements,” *Treatise on Geochemistry* **2**, 61–101 (2003).
- A. J. Irving, “A review of experimental studies of crystal/liquid trace element partitioning,” *Geochim. Cosmochim. Acta* **42**, 743–770 (1978).
- M. G. Jackson, R. A. Cabral, E. F. Rose-Koga, K. T. Koga, A. Price, E. H. Hauri, and P. Michael, “Ultra-depleted melts in olivine-hosted melt inclusions from the Ontong Java Plateau,” *Chem. Geol.* **414**, 124–137 (2015).
- P. B. Kelemen and K. Høghøj, “One view of the geochemistry of subduction-related magmatic arcs, with an emphasis on primitive andesite and lower crust,” *Treatise on Geochemistry* **3**, 593–659 (2003).
- V. I. Kovalenko, V. B. Naumov, A. V. Girmis, V. A. Dorofeeva, and V. V. Yarmolyk, “Volatiles in basaltic magmas of ocean islands and their mantle sources: II. Estimation of content in mantle reservoirs,” *Geochem. Int.* **45** (4), 313–326 (2007).
- Y. Li and A. Audetat, “Partitioning of V, Mn, Co, Ni, Cu, Zn, As, Mo, Ag, Sn, Sb, W, Au, Pb, and Bi between sulfide phases and hydrous basanite melt at upper mantle conditions,” *Earth Planet. Sci. Lett.* **355–356**, 327–340 (2012).
- Y. Li and A. Audetat, “Gold solubility and partitioning between sulfide liquid, monosulfide solid solution and hydrous mantle melts: Implications for the formation of Au-rich magmas and crust–mantle differentiation,” *Geochim. Cosmochim. Acta* **118**, 247–262 (2013).
- Y. Li and A. Audetat, “Effects of temperature, silicate melt composition, and oxygen fugacity on the partitioning of V, Mn, Co, Ni, Cu, Zn, As, Mo, Ag, Sn, Sb, W, Au, Pb, and Bi between sulfide phases and silicate melt,” *Geochim. Cosmochim. Acta* **162**, 25–45 (2015).
- J. Maclennan, “Lead isotope variability in olivine-hosted melt inclusions from Iceland,” *Geochim. Cosmochim. Acta* **72**, 4159–4176 (2008).
- D. McKenzie and R. K. O’Nions, “Partial melt distributions from inversion of rare earth element concentrations,” *J. Petrol.* **32**, 1021–1091 (1991).
- V. B. Naumov, V. A. Dorofeeva, A. V. Girmis, and V. A. Kovalenko, “Volatile, trace, and ore elements in magmatic melts and natural fluids: evidence from mineral-hosted inclusions. I. Mean concentrations of 45 elements in the main geodynamic settings of the Earth,” *Geochem. Int.* **60** (4), 325–344 (2022).
- H. Palme and H. St. S. O’Neill, “Cosmochemical estimates of mantle composition,” *Treatise on Geochemistry* **3**, 1–39 (2014).
- J. A. Pearce and D. W. Peate, “Tectonic implications of the composition of volcanic arc magmas,” *Annu. Rev. Earth. Planet. Sci.* **23**, 251–285 (1995).
- R. L. Rudnick and S. Gao, “Composition of the continental crust,” *Treatise on Geochemistry* **4**, 1–51 (2014).
- J. G. Ryan and C. H. Langmuir, “The systematics of boron abundances in young volcanic rocks,” *Geochim. Cosmochim. Acta* **57**, 1489–1498 (1993).
- V. J. M. Salters and A. Stracke, “Composition of the depleted mantle,” *Geochem., Geophys., Geosyst.* **5** (5), 1–27 (2004).
- A. V. Sobolev and N. Shimizu, “Ultra-depleted primary melt included in an olivine from the mid-Atlantic ridge,” *Nature* **363**, 151–154 (1993).
- A. Stracke, “Earth’s heterogeneous mantle: A product of convection-driven interaction between crust and mantle,” *Chem. Geol.* **330–331**, 274–299 (2012).
- B. J. Wood and J. D. Blundy, “Trace element partitioning: The influences of ionic radius, cation charge, pressure, and temperature,” *Treatise on Geochemistry* **3**, 421–448 (2014).

Translated by E. Kurdyukov